Monitoring Wind Turbine Loading Using Power Converter Signals

C.A. Rieg[a], C.J. Smith[a], C.J. Crabtree[a],

[a]Energy Group, School of Engineering and Computing Sciences, Durham University

I. Introduction

Extreme wind conditions, such as gusts, result in large load differences on the turbine that can be damaging to mechanical components such as the gearbox [1]. In response, the condition of wind turbine components is monitored so that a developing fault can be detected and appropriate action taken. This allows maintenance to be scheduled before the impact on the system has become too large, resulting in lower downtimes and lower cost of energy (CoE) [2].

Condition monitoring (CM) techniques such as vibration and strain measurement require expensive sensors that are often impractical in high-torque applications of wind turbines [3]. Using readily available signals from other areas of the turbine could prove an inexpensive alternative approach to CM.

The power converter could provide this information for CM applications; the converter should respond to any disturbances and therefore its signals should show the drive train response. For example, the quadrature-axis component of the machine side converter (MSC) current signal (I_q) controls the real power flow and contains torsional information from the drive train. Monitoring I_q could provide useful information about torsional loads on components that could be used for early fault detection without extra sensors.

This investigation focuses on whether power converter signals can be used for CM with a focus on two potential applications:

1. Gear tooth failure detection.
2. Mechanical load estimation from damaging gusts.

II. Approach

To carry this work out a drive train model was required. The model developed at Durham in [4] was used. To make this model suitable for this study the following modifications were made:

a. A full grid-side converter (GSC) was added.
b. A gearbox was added.
c. A gearbox fault model was used to provide fault conditions.
d. A gust model was added to provide data for load prediction.

This section outlines how these aspects were modelled.

a. Grid-Side Converter

The main objective of the GSC is to control power flow between converter and grid to maintain a constant DC link voltage. In the drive train model the GSC is modelled as a 2-level insulated-gate bipolar transistor (IGBT)/diode pair inverter.

To control the GSC, vector control was chosen [5]. Figure 1 outlines the control procedure for the GSC. I_d is the direct-axis current, V_d is the direct-axis voltage, ω is the grid frequency (rad/s), L is grid inductance, V_{DC_link} is the DC-link voltage, V_q is the quadrature-axis voltage and V_0 is the 0-component voltage.

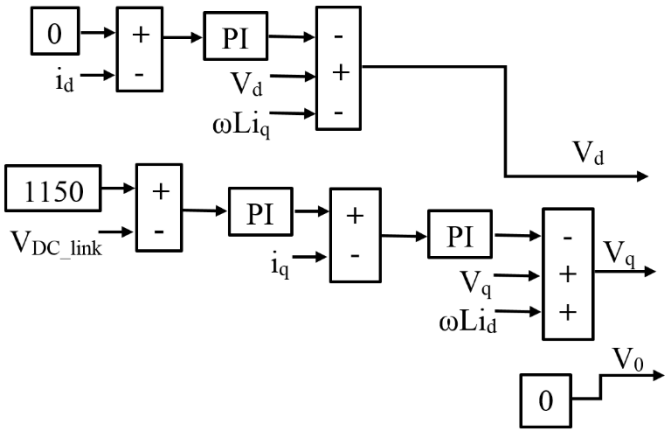

Figure 1- Vector control scheme for the GSC

b. Gearbox model

The gearbox is connected to the hub via the low-speed shaft and to the generator via the high-speed shaft. The dynamic interactions of the rotor, gearbox and generator were modelled as a 3-mass model shown in Figure 2.

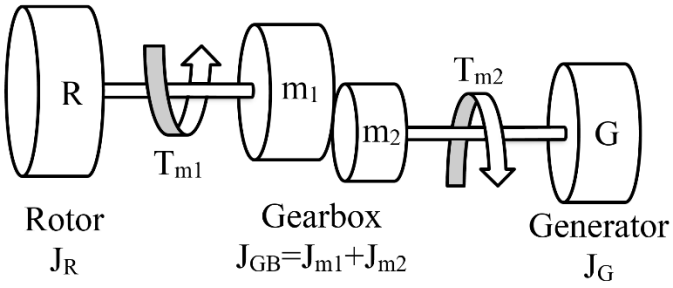

Figure 2- Schematic of the 3-mass model dynamics

J_R is the rotor moment of inertia, J_{GB} is the gearbox moment of inertia, $J_{m1,2}$ are the equivalent moments of inertia for the low and high speed gear sections respectively, $T_{m1,2}$ are the equivalent mechanical torques for the low and high shafts respectively and J_g is the generator moment of inertia.

c. Gearbox fault model

The most severe gearbox failure modes that arise from extreme wind conditions have been identified as fretting corrosion and high cycle bending fatigue [6]. Fretting corrosion is the deterioration of contacting gear tooth surfaces as a result of vibratory motion between teeth and has been set as the study's focus.

Gear tooth wear causes a reduction in the gear stiffness. This reduction of the gear contact stiffness in the faulty gear can be applied to gear models that include a stiffness component and can be modelled as a rectangular pulse wave or a half sine function [7]. For this study the rectangular pulse function was chosen and applied to the high-speed shaft.

Figure 3 shows the variation in total stiffness when a fault is present.

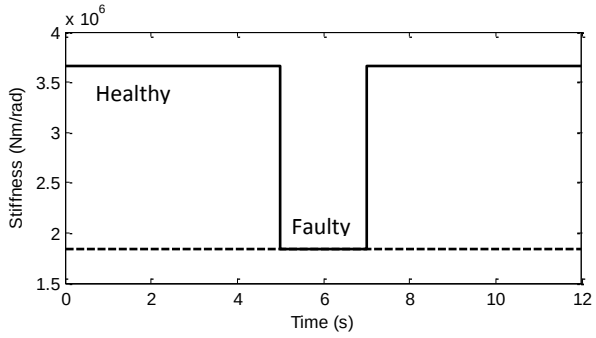

Figure 3- Stiffness variation with a worn gear

d. Gust model

Previous gust models rely on real wind data to model the amplitude, duration and gust shape introduced along with a running average wind speed [8, 9]. These wind gust profile characteristics can be extracted and applied using square or cosine shaped wind profiles that have a gust amplitude, duration and frequency. The maximum gust speed ($U_{G,max}$) in a given time period is calculated from the gust factor $G(t)$ (1). An expression for the gust factor is given in (2) [10].

$$U_{G,max} = G(t)U_W \quad (1)$$

$$G(t) = 1 + 0.42I_u \ln\frac{3600}{t} \quad (2)$$

Where U_w is the mean wind speed, I_u is the longitudinal turbulence intensity, and t is the gust duration.

For this study the underlying square wave gust characteristic was used. For the load prediction model gust, 10 gust categories were defined, each representing a reduction in the gust wind speed (Table 1).

Gust Category	U_G
1	$(U_G+U_W) + U_W$
2	$[(U_G + U_W)/1.25] + U_W$
3	$[(U_G + U_W)/1.5] + U_W$
4	$[(U_G + U_W)/1.75] + U_W$
5	$[(U_G + U_W)/2] + U_W$
6	$[(U_G + U_W)/2.25] + U_W$
7	$[(U_G + U_W)/2.5] + U_W$
8	$[(U_G + U_W)/3] + U_W$
9	$[(U_G + U_W)/4] + U_W$
10	$[(U_G + U_W)/6] + U_W$

Table 1 - Gust category assignment

III. Results

a. Gearbox Fault Detection

Gearbox wear faults were introduced using the previously detailed method. The first fault was a wear fault with amplitude 0.5 and length 1mm present on every other tooth with a constant wind speed of 7m/s.

The frequency spectrum of the MSC I_q signal was computed using the Fast Fourier Transform to identify differences between the 'healthy' (no fault) and faulty spectrum (Figure 4). It can be seen that there is no clear difference in the spectrum at the fault frequency. There is a small difference at 2Hz, where both the healthy and the faulty spectrum show a spike due to the wind input.

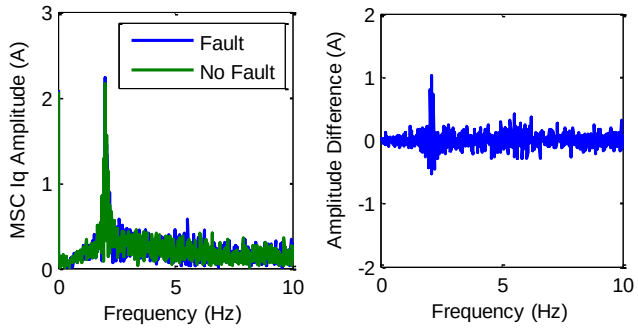

Figure 4 – MSC I_q frequency response

The lack of fault signal was investigated by inspecting the frequency spectrum of the stiffness and damping torque components in isolation ($T_{k,\ B}$) (figure 5). The fault is visible in the T_K and T_B spectra but not in the resulting torque spectrum. The time sequences showed that the oscillatory motion of T_K due to the fault is counteracted by an opposite oscillatory motion from T_B removing the oscillation from the frequency spectrum.

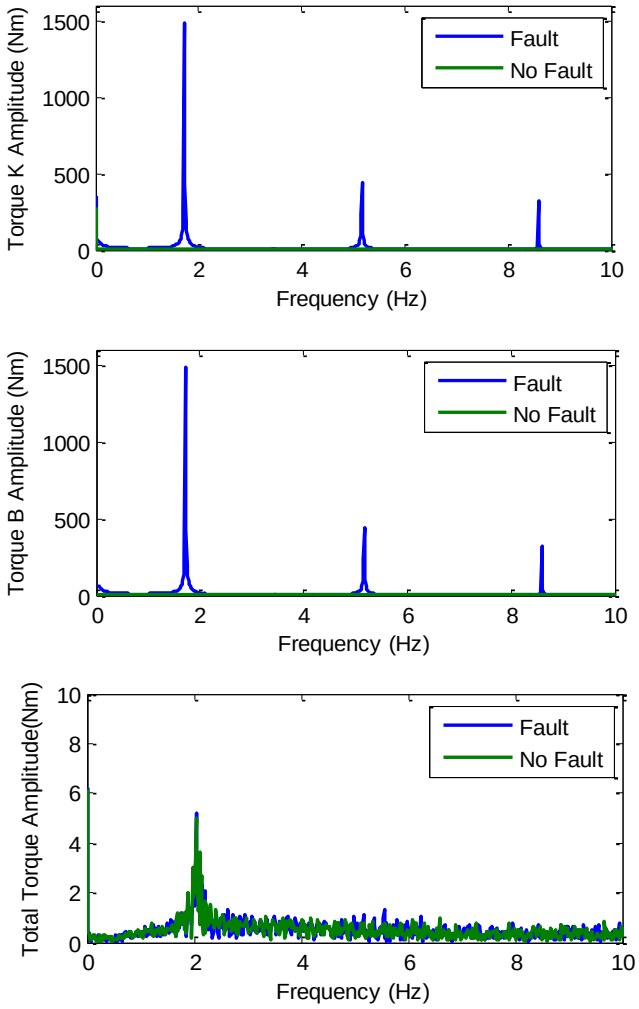

Figure 5 – Frequency spectrum of mechanical torque

In a real gearbox the damper and stiffness torque components cannot be measured separately. However, in a real gearbox the system parameters might not be as balanced. Thus there is still a possibility that faults can be detected in the MSC I_q signal of a real gearbox system.

b. Load prediction on mechanical components using MSC signals

The first task was to determine whether there was a relationship between MSC I_q and rotor torque for different gust categories (GC). Simulations were carried out at different speeds with a constant gust frequency of 3Hz and the change in rotor torque (ΔT_r) and ΔI_q were recorded. The results for the first three gust categories are shown in Figure 6.

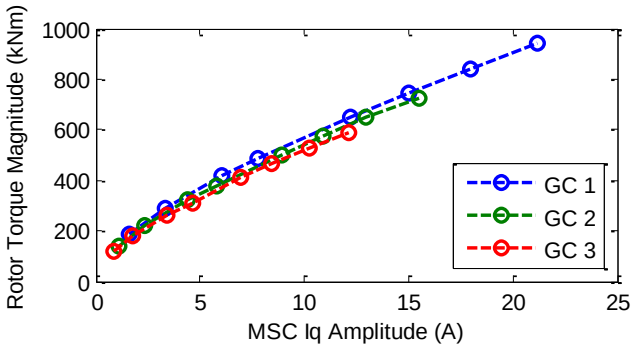

Figure 6 – Change in rotor torque vs MSC I_q amplitude for different gust categories.

Figure 6 shows that the GC each have a separate relationship. These relationships can therefore be used to determine the mechanical loading from the mean wind speed, gust magnitude and MSC signal amplitudes. The load prediction model is outlined in Figure 7.

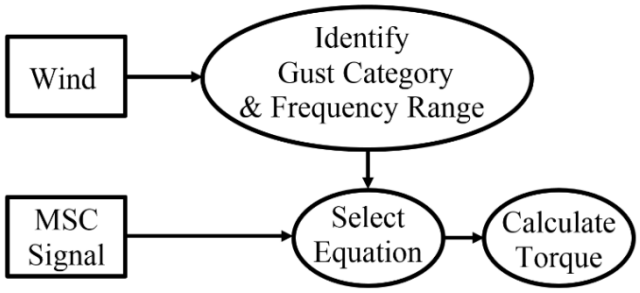

Figure 7 - Flowchart of the load prediction model

To verify this method a number of category 1 gusts with different U_w were introduced, I_q was measured and the above relationships were used to determine the estimated loading. The results are summarised in Table 2.

U_W (m/s)	MSC I_q (A)	ΔT_r (Nm) calc.	ΔT_r (Nm) meas.	Estimation Error (%)
5.5	4.536	353636.5	350370	0.93
6.2	6.648	448868.5	445450	0.8
7	9.84	573264.2	568160	0.9
8.2	16.344	786715	780330	0.81

Table 2 - Model Verification

The % error between the measured and calculated ΔT_r is <1%. Therefore the model is able to predict accurately the mechanical components' loading using MSC signals.

IV. Conclusion

CM of wind turbine components allows appropriate action to be taken to minimise the impact of developing fault but currently requires expensive sensors and data acquisition devices**.** In response, this paper outlines an investigation into whether converter signals, which are already monitored, can be used for CM.

A drive train model was modified to include a gearbox, GSC and gearbox fault model to determine whether gearbox faults could be detected in the converter signals. Gusts were also modelled to determine if drive train mechanical loading could be predicted using converter signals. The conclusions from this study are:

- Gear wear cannot be detected in the MSC signals due to the model damping effects.
- A model using MSC signals successfully predicted the load changes in the turbine with a percentage error < 1%.

Further investigations into the magnitude of load changes that cause mechanical component damage could lead to the application of this accurate MSC-based load prediction model to prevent gearbox faults through turbine shutdown during damaging wind conditions.

V. Learning objectives

The learning objectives are as follows:

- To explore the use of converter signals for CM of gearboxes without extra sensors.
- To determine whether gearbox faults are detectable in the converter current signals.
- To develop a turbine load prediction model using converter current signals.

VI. References

[1] Kanev, S. van Engelen, T. *Wind Turbine Extreme Gust Control.* Wind Energy, vol. 13, pp. 18-35, 2010.

[2] Han, Y. Song, Y. H. *Condition Monitoring Techniques for Electrical Equipment—A Literature Survey*. IEEE Transactions on Power Delivery, Vol. 18, No. 1, pp4-13, 2003.

[3] Yang W, Tavner P.J., Crabtree C.J., Wilkinson M. *Cost-effective condition monitoring for wind turbines*. IEEE transactions on industrial electronics, 57 (1), pp. 263-271, 2010.

[4] Smith C.J.; Wadge G.N.; Crabtree C.J.; Matthews P.C. *Characterisation of Electrical Loading Experienced by a Nacelle Power Converter*. EWEA Conference, Paris, France, November 2015.

[5] Anaya-Lara O, Jenkins N, Ekanayake J, Cartwright P, Hughes M. *Wind Energy Generation: Modelling and Control.* West Sussex, UK, 2009.

[6] Sheng S, McDade M. *Wind Turbine Failure Modes – A Brief.* Los Angeles, California, 2011.

[7] Cui L, Cai C. *Nonlinear Dynamics of a Gear-Shaft-Bearing System Breathing Crack and Tooth Wear Faults.* The Open Mechanical Journal, pp. 483-491, Shanghai, China, 2015.

[8] Sheridan P. *Review of techniques and research for gust forecasting and parameterization.* Forecasting Research Technical Report 570, April 2011. Available at: http://www.metoffice.gov.uk/media/pdf/e/3/FRTR570_Tagged.pdf.

[9] Verheij F, Cleijne J, Leene J. *Gust Modelling for Wind Loading*. Journal of Wind Engineering and Industrial Aerodynamics, vol. 42, no. 1-3, pp. 947-958, Oct. 1992.

[10] Burton T, Jenkins N, Sharpe D, Bossanyi E. *Wind Energy Handbook*. Second Edition, Wiley, 2011.